Influence of nanosized magnesia on the hydration of borehole-sealing cements prepared using different methods

Quanle Zou[1] · Jinfei Zhan[1] · Xin Wang[1] · Zhen Huang[1]

Abstract

Gas drainage is an effective technology for gas control in coal mines. A high borehole-sealing quality is the fundamental precondition for efficient gas drainage. The expansibilities of cement pastes used in borehole-sealing processes are critical for the borehole-sealing effect. Nanosized magnesia expansive agents are used to improve the expansibilities of cement pastes and improve the borehole-sealing effect. Nuclear magnetic resonance spectrometry and scanning electron microscopy were adopted to study the effects of nanosized magnesia on the hydration of borehole-sealing cements used with different preparation methods. The results showed that an increase in the mass fraction of the nanosized magnesia promoted cement hydration, and the mass fraction was positively correlated with the promotion effect. The use of different preparation methods did not change the water-phase distribution in the cement. When using the wet-mixing preparation method, nanosized magnesia promoted the induction, acceleration, and deceleration periods of hydration; when using the dry-mixing preparation method, the nanosized magnesia promoted the induction period of cement hydration, and the promotion effect was less obvious than that seen when using the wet-mixing method. When using the wet-mixing preparation method, the nanosized magnesia was uniformly dispersed, thus enlarging the surface area of the reaction, which provided more nucleation sites for the hydration products of the cement and therefore accelerated the hydration reaction. When using the dry-mixing preparation method, the nanosized magnesia powders were dispersed nonuniformly and aggregated. Under these conditions, only a few nanosized magnesia particles on the surfaces of the aggregated clusters took part in hydration, so only a small number of nucleation sites were provided for the hydration products of cement. This led to inconsistent hydration of cement pastes prepared using the dry-mixing method. The surface porosity of the cement prepared with the wet-mixing preparation method first decreased and then increased with increases in the mass fraction of the nanosized magnesia. The cement surface exhibited compact hydration products and few pores, and the surface was relatively smooth. In comparison, the surface porosity of the cement prepared using the dry-mixing method fluctuated with increasing mass fraction of the nanosized magnesia, resulting in a rough cement surface and microfractures on some surfaces. The two preparation methods both reduced the surface porosity of the cement. The wet-mixing preparation was more effective and consistent in improving the compactness of the cement than the dry-mixing preparation. These results provide important guidance on the addition of nanosized magnesia in borehole-sealing engineering and the selection of cement preparation methods, and they also lay a solid foundation for realizing safe and efficient gas drainage.

Keywords Borehole-sealing cement · Nanosized magnesia · Preparation method · Hydration · Morphological analysis · Nuclear magnetic resonance relaxation analysis

✉ Quanle Zou
quanlezou2011@126.com

✉ Xin Wang
wangxin991129@163.com

1 State Key Laboratory of Coal Mine Disaster Dynamics and Control, School of Resources and Safety Engineering, Chongqing University, Chongqing 400044, China

1 Introduction

As shallow resources have gradually been exhausted, mining has been extended to greater depths (Ran et al. 2023a; Zou et al. 2022; Zhang et al. 2009). Deep coal mining leads to major problems in controlling coal and gas outburst disasters (Zou et al. 2023; Zhai et al. 2016; Xie et al. 2019). Gas predrainage from boreholes is the

main technology used to control gas disasters and enable efficient utilization of gas resources (Ran et al. 2023b; Lu et al. 2022). In most mines in China, the concentrations of gas drained from boreholes are low, and the net gas yields are not high. The quality of the borehole-sealing process directly affects gas drainage (Liu et al. 2014; Ge et al. 2015; Wang et al. 2016). At present, the sealing materials used for gas drainage boreholes include cement-based, polyurethane, and polymer materials. Due to its characteristics, including short setting times, high strength, and favourable impermeability, cement has been widely used in grouting and sealing engineering (Yan 2014).

The properties of borehole-sealing materials directly influence the borehole-sealing quality. Additives to borehole-sealing cement-based materials improve their comprehensive properties, improve the borehole-sealing quality and ensure efficient gas drainage (Ma et al. 2014). Nanosized materials exhibit excellent properties, including surface effects, small sizes, high activities, and complex functions, due to their special scale; therefore, they have received much attention in numerous studies of cement-based materials. At present, scholars have conducted many studies on the use of nanosized materials in cement. Ren et al. (2021) investigated the effects of nano-silica, nano-titanium oxide and nano-calcium oxide on the early hydration and mechanical properties of Portland cement at small doses, and optimized the amounts of the three nanomaterials by response surface methodology. The results showed that the addition of nanomaterials could greatly promote the hydration of Portland cement and improve its early compressive strength. Wang and Duan (2013) investigated the flowability and mechanical properties of grouting materials with different cement-sand ratios and the effect of nano-silica on the properties of grouting materials, and came up with the optimal ratio. Farzadnia et al. (2013a, b, c) noted that nanosized clay to mortars improved the performance of cement composites, which showed a pozzolanic reaction with cement and the microaggregate filling effect (Aly et al. 2011; Hakamy et al. 2013). Meanwhile, previous research also found that the addition of nanosized titanium dioxide and nanosized aluminium oxide to cement enhanced the mechanical properties and energy absorption of the cement (Farzadnia et al. 2013a, c). Nanosized calcium carbonate particles provide nucleation sites for hydration products and ultimately improve hydration. Additionally, the particles are nanofillers and improve the mechanical performance of the cement composite (Liu et al. 2012; Supit and Shaikh 2014; Sato and Diallo 2018). In addition, Nazari and Riahi (2011) showed experimentally that nanosized zinc peroxide and nanosized titanium dioxide powders improved the mechanical and physical performance of cements. All of these results suggest that nanosized materials have many applications in cement-based materials and have effectively improved their performance.

Nanosized magnesia (MgO) expansive agents have frequently been used in engineering high-performance cement concrete due to their many advantages, including low consumption in hydration, stable hydration products, and easy active regulation of expansion. They solve the problem of self-constriction seen with hardened cement pastes. Moradpour et al. (2013) found that a MgO nanosized filler significantly strengthened the internal structures of cement composites and significantly improved the strengths. Ye et al. (2015) believed that nanosized MgO improved the long-term strength of cement and could also be used as a cement expansive agent. Gao et al. (2015) noted that nanosized MgO enhanced the strength and stability of cement and increased cementation and pore filling. Hou et al. (2017) showed that the use of nanosized MgO shortened the initial setting and final setting times of cement, and its impact on cement hydration changed dramatically with changes in the water-cement ratio. Existing research on the effects of nanosized MgO on cement has mainly been focused on the strength and stability of the modified cement, and there is a lack of research on the effect of nanosized MgO on cement hydration.

The kinetics of the cement hydration process is one of the important aspects of cement chemistry. Particularly in the early stage of hydration, the compositions of the cement pastes and the microstructures formed exert important effects on the performance of the hardened cement. Several test methods have been used to study the cement hydration process, such as calorimetry (Sun et al. 2006), ultrasonic treatments (Xiao and Li 2008), and electrical resistivity measurements (Nestle 2004). These methods characterize the cement hydration process by tracking the physical and chemical changes related to hydration progress, such as hydration-induced heat release, as well as changes in the viscoelasticity, porosity, and ionic concentration. Water is an essential component in cement paste, and the state changes of water are among the key steps of hydration. As hydration continues, water changes from free water to chemically bound water, physically absorbed water, and pore water. The hydration process can be studied by exploring signals for protons in water exhibiting different binding states, and nuclear magnetic resonance (NMR) is the method used to study cement hydration (Bohris et al. 1998). NMR can be used for nondestructive, continuous and repeated tests of the same cement sample, and the state of water in the cement paste is determined by by measuring T_1 and T_2 relaxation time. Therefore, NMR was used in this study to explore the hydration processes of cement pastes modified with nanosized MgO, which is important for determining the impact of the nanosized MgO on cement hydration.

Nanosized materials must be dispersed when used in cement-based materials because the particle sizes and high surface energies of the powdered particles and sols lead to aggregation in aqueous solutions. The nanosized materials can be added to compositions as dry powders or as aqueous solutions. Kritikaki et al. (2009) investigated the effect of alumina nanoparticles on ceramic microstructure, porosity and flexural strength under different mixing methods, and the results of the study showed that the strength was higher when added in the gel state than in the dry powder state. Horszczaruk et al. (2020) investigated the effect of dispersion methods on the homogeneous quality of nano-dopants in cement matrices and showed that a combination of mechanical methods (e.g. ultrasonic and/or high-speed mixing) and chemical modifications (functionalisation or coating) can achieve effective dispersion of nanomaterials in cement matrices. Therefore, the mixing and preparation methods used with nanosized materials and cement-based materials are important for applications of field-modified cements.

Prior research on the effects of nanosized MgO on cement have mainly been focused on the strengths and stabilities of the modified cements. However, there is a lack of research on the overall hydration process for borehole-sealing cement when nanosized MgO is used with different preparation methods. Therefore, this research was designed to reveal the phase changes occurring in water during hydration of cement modified with nanosized MgO, and different preparation methods and different mass fractions of nanosized MgO were used to study their impacts on the hydration of borehole-sealing cement. Microscopic analyses of the hydration products were also used to probe the mechanism by which the nanosized MgO affected cement hydration, which provided a theoretical basis for pumping borehole-sealing cement in the field and enabled the use of nanosized MgO in borehole-sealing engineering.

2 Sample preparation and test methods

2.1 Test materials and sample preparation

Class-G high sulfate-resistant cement was used in the tests, which is applicable to most well-cementing operations after blending with additives. The nanosized material used in the tests was nanosized MgO with an average particle size of 20 nm. It was a white fluffy powder with a purity of at least 99.99% and a specific surface area of 120 m^2/g.

Two methods were used to prepare cements modified with nanosized MgO. In the wet-mixing preparation,

nanosized MgO was used to prepare an aqueous solution, which was stirred uniformly using a glass rod; then, the solution was placed in an ultrasonic instrument to prepare a nanofluid, which was then mixed with cement to prepare the cement paste. In the dry-mixing preparation, the nanosized MgO powder was mixed uniformly with the cement, and then water was added and stirred to prepare a cement paste. The same mass of class-G cement was mixed with water to give a water-cement ratio of 0.44. Afterwards, nanosized MgO with mass fractions of 0‰, 1‰, 2‰, 3‰, and 4‰ was separately added to prepare 10 cement pastes with the above two methods. The cement pastes prepared using the wet-mixing method were labelled N1, N2, N3, N4, and N5, and those prepared using the dry-mixing method were labelled M1, M2, M3, M4, and M5. The preparation methods are illustrated in Fig. 1.

2.2 Test methods

The test methods are shown in Fig. 2. First, NMR was used to test the T_2 values of the 10 prepared cement pastes after hydration for 5, 30, 60, 120, 240, 720, 1200, and 1800 min. Then, scanning electron microscopy (SEM) was used to observe the micromorphologies of the hardened cement pastes.

The NMR studies of relaxation times mainly involved the longitudinal relaxation time T_1 and the transverse relaxation time T_2. T_2 reflects the freedom of the water, interactions of different water phases, and influence of the ionic concentration on the surrounding environment, the polymer, and the pores. Water in different states exhibits different T_2 values (Holly et al. 2007; Simina et al. 2012; Tavassolian et al. 2014; Behroozmand et al.T 2015). The NMR instrument used in the research was a low-field NMR spectrometer produced by Suzhou NiuMag Analytical Instrument Corporation. The magnetic field intensity of the permanent magnet, the magnetic field homogeneity, the stability of the magnetic field, and the temperature of the magnet were 0.53 T, 3×10^{-4}, less than 300 Hz/h, and a constant 32℃. Before sampling, CPMG pulse sequences were used, and the echo time (TE) was 0.2 ms, the number of echoes (NECH) was 5000, and the number of scans (NS) was 8. The collected relaxation data were treated with inversion software to obtain the T_2 distribution curves of the samples. The hardened cement pastes were prepared into samples with lengths of 10 mm and widths of 5 mm. After metal spraying, a scanning electron microscope was used to observe the micromorphologies of the hardened cement pastes.
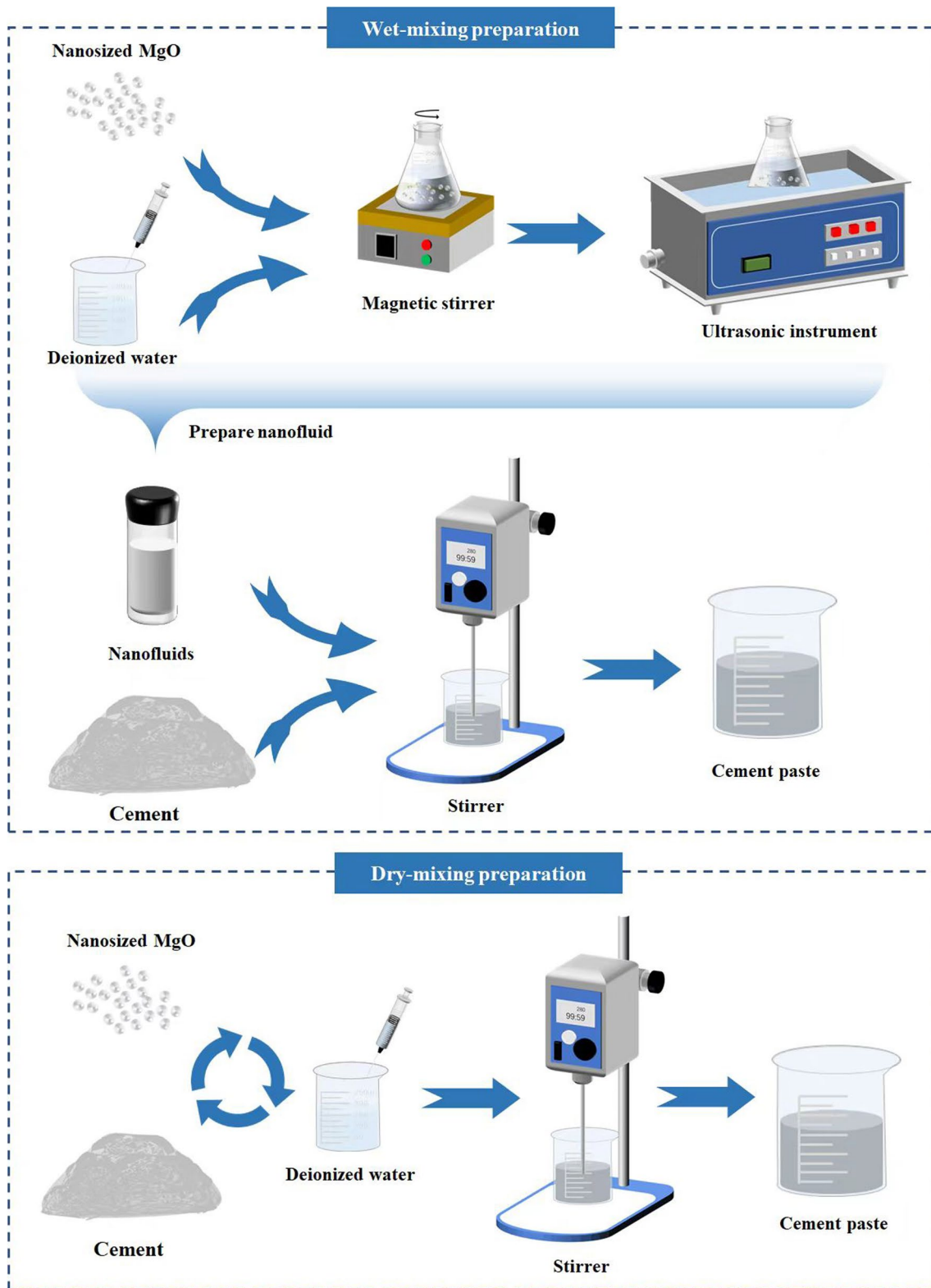
Fig. 1 Cement pastes prepared with different methods

Fig. 2 Test processes

① **NMR test**　② **SEM observation**

3 Results

3.1 Time evolution of the transverse relaxation peaks

3.1.1 Time evolution of the relaxation peaks for cements prepared with the wet-mixing method

The sealing cement material is mainly composed of cement clinker particles, and after adding water, hydration reaction occurs rapidly. As the hydration reaction continues, a hardened cement slurry is eventually formed, with the highest free water content in the slurry at the time when the cement and water start to mix, followed by the conversion of the free water injection to physically bound and chemically bound water along with the hydration reaction. In explaining fluid relaxation in pore media, the commonly applied model for confined fluids, also known as the BT model, was developed by Brownstein and Tarr (1979). According to the NMR principle, the transverse relaxation time T_2 spectrum distribution can reflect the degree of water freedom and the pore size and distribution of the hardened slurry, and the pore size is related to the position of the relaxation peak. The smaller pore group corresponds to smaller T_2 values and the larger pore group corresponds to larger T_2 values, respectively. The movement of the relaxation peak can reflect the changing law of water freedom and the changing law of pore space of the hardened slurry during the hydration process of cement. The relaxation peak area and peak apex reflect the changes of pore volume and quantity in the cement-hardened slurry (Behroozmand et al. 2015).

The T_2 distribution curves measured after 5, 30, 60, 120, 240, 720, 1200, and 1800 min for various cement pastes prepared with the wet-mixing method are illustrated in Fig. 3. When the hydration duration was 5–240 min, the relaxation peaks of the cement shifted to shorter relaxation time as the mass fraction of nanosized MgO was increased. In addition,
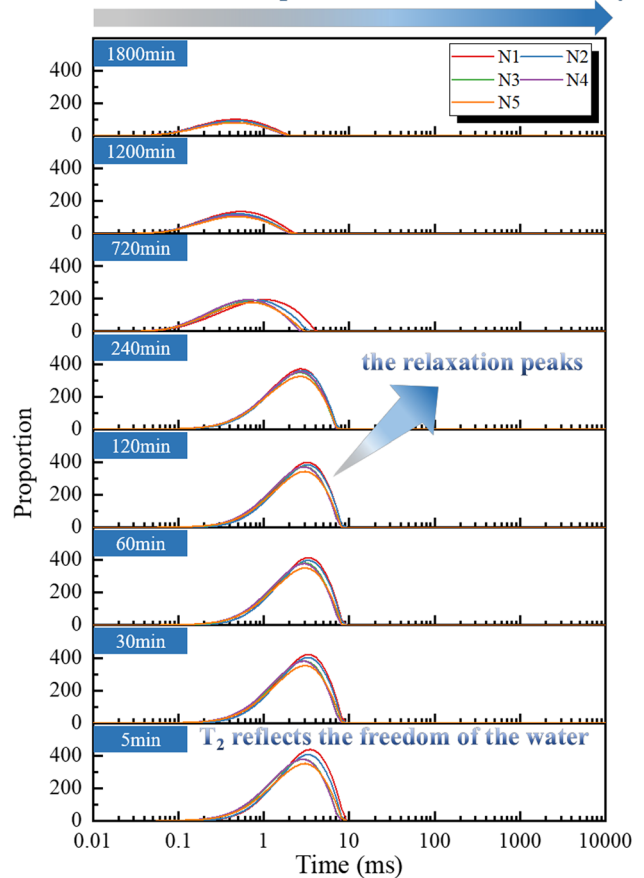

Fig. 3 T_2 distribution curves measured during hydration of various cement pastes prepared using the wet-mixing method

the peak intensities also decreased, and the relaxation peaks also narrowed. As the hydration process continued for 720 min, the positions of the relaxation peaks continued to shift leftward with increasing MgO mass fraction. The shifts were more obvious than those seen in the early hydration period.

In addition, the relaxation peaks shifted toward shorter relaxation times, with lower peak intensities and smaller peak areas. The relaxation peak shapes also varied more than they did in the early hydration period, and the peaks shifted obviously toward shorter relaxation time. After hydration for 1200 min, the relaxation peaks for the various cement pastes shifted further to shorter relaxation times of 0.1–1 ms, and peaks appeared at 0.5 ms. After hydration for 1800 min, the relaxation peaks for the various cement pastes declined to the minimum for the overall test period. With increases in the mass fraction of nanosized MgO, the areas and values of the relaxation peaks both decreased gradually, and the positions of the relaxation peaks gradually shifted to shorter relaxation times.

3.1.2 Time evolution of the relaxation peaks for cements prepared using the dry-mixing method

The T_2 distribution curves measured after 5, 30, 60, 120, 240, 720, 1200, and 1800 min for various cement pastes prepared with the dry mixing process are displayed in Fig. 4. The evolution characteristics of the relaxation peaks fo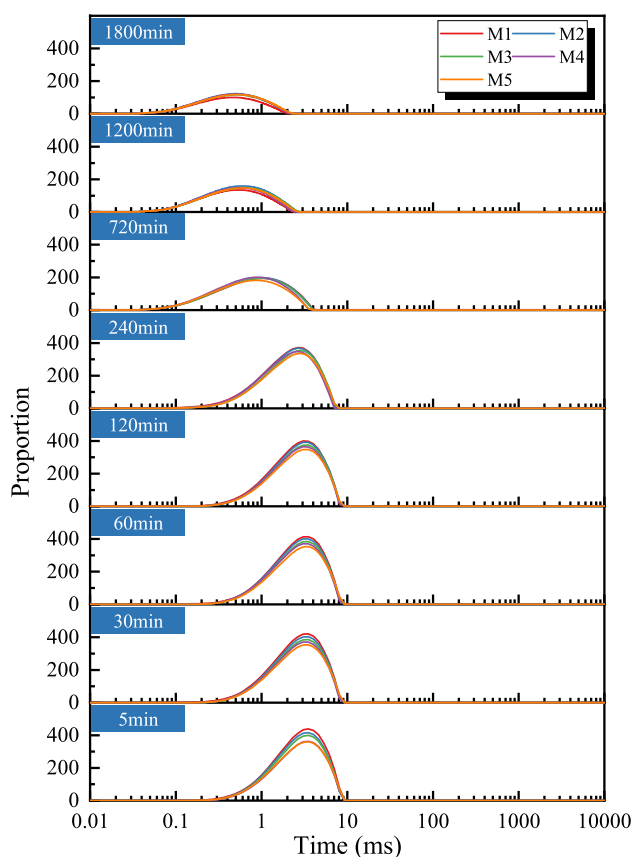r the cements prepared with the dry-mixing method were similar to those of the cements prepared with the wet-mixing method. Within 720 min of hydration, the T_2 distributions for samples M1 to M5 all exhibited similar trends with increasing in mass fractions of nanosized MgO, and the relaxation peak areas tended to shrink. The relaxation peaks gradually shifted to shorter relaxation times, with lower peak intensities and smaller peak areas. The relaxation peaks constantly narrowed with longer relaxation times, while those with shorter relaxation times were enlarged. The relaxation times decreased, and the relaxation peaks were distributed more closely. This indicated that when using the dry-mixing preparation method, the addition of nanosized MgO can also enhanced hydration of the cement pastes, and the extent of enhancement increased as the mass fraction of the nanosized MgO was increased. When the hydration times were 1200 and 1800 min, the relaxation peaks for the cement pastes prepared with different mass fractions of the nanosized MgO changed in different ways. This suggested that when using the dry-mixing preparation method, the extent to which the nanosized MgO enhanced hydration of the cement pastes was inconsistent.

3.2 Changes in the overall relaxation signals

3.2.1 Changes in overall relaxation signals of cement pastes prepared with the wet-mixing method

From the above principle of NMR relaxation analysis, it is clear that the distribution of transverse relaxation time T_2 can reflect the free degree of water and the pore size of the hardened slurry during the hydration process of the cement. The total T_2 values measured for the various cement pastes at different times in the hydration process were subjected to
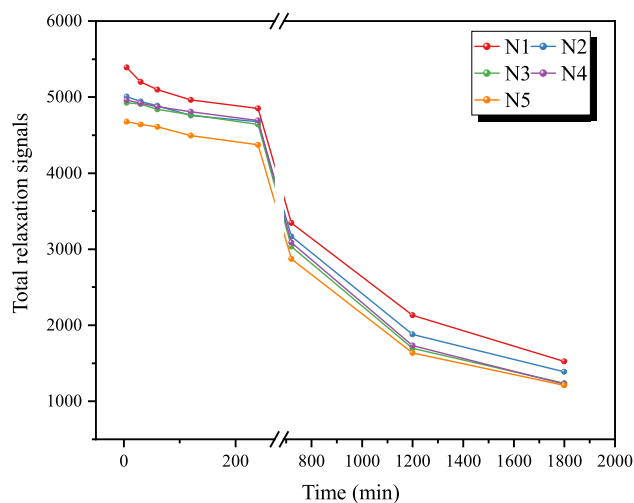

Fig. 4 T_2 distribution curves measured during the hydration of various cement pastes prepared with the dry-mixing method

Fig. 5 Total relaxation signals as a function of time for the cement pastes prepared with the wet-mixing method

statistical analyses to determine the relaxation times of water and hydrates in the cement pastes, as shown in Fig. 5. As hydration proceeded, the cement pastes with different mass fractions of nanosized MgO exhibited similar change trends. The total relaxation signals for the various cement pastes always declined gently at first, then decreased significantly, and decreased slowly with increasing hydration time. Within the hydration times of 0–240 min, the total relaxation signals of the various cement pastes decreased gradually. Within 240–1200 min of hydration, the changes in the total relaxation signals increased, and the rate accelerated more than that for the previous stage. Within 1200–1800 min of hydration, the reductions in the total relaxation signals for the various cement pastes gradually slowed, and the changes in the total relaxation signals became gentle again. If the whole hydration process was monitored, the total relaxation signals for the various cement pastes showed decreasing trends. When the hydration time was 1800 min, the total relaxation signals for the various cement pastes reached the minimum for the entire hydration process, and they always decreased with increases in the mass fraction of the nanosized MgO.

3.2.2 Changes in total relaxation signals of cement pastes prepared using the dry-mixing method

Figure 6 shows the changes observed in the total relaxation signals of the cement pastes prepared with the dry-mixing method. The total relaxation signals of the showed changes similar to those seen for samples prepared with the wet-mixing method. As hydration proceeded, the total relaxation signals of the cement pastes tend to decrease. Within 0–240 min of hydration, the total relaxation signals of the various cement pastes decreased gently. When the hydration duration
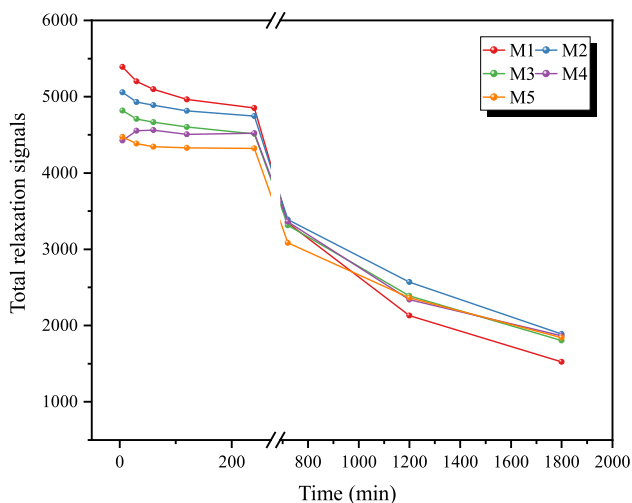

Fig. 6 Total relaxation signals as a function of time for the cement pastes prepared with the dry-mixing method

was 240–1200 min, the total relaxation signals of the various cement pastes decreased rapidly. Within 1200–1800 min of hydration, the decreasing trend for the total relaxation signals of the various cement pastes became gentle again.

3.3 Changes in the micromorphologies of the hardened cement pastes

The micromorphologies of the various hardened cement pastes are illustrated in Fig. 7. When observed with a magnification of 500 times, samples N1–N5 showed smooth surfaces, samples N1 and N2 showed asperities and pits on the surfaces, and samples N3–N5 had smooth surfaces. After amplification at 5000 times, samples N1–N5 exhibited many folds on the surfaces, the surfaces of samples N1 and N2 became rough, and samples N3–N5 had regular surfaces on which fine particles appeared. After amplification at 10,000 times, particles were clearly visible on the surfaces of samples N1–N5; there were many folds on the surfaces of samples N1 and N2, on which numerous pores were observed; the surfaces of samples N3–N5 were smooth, and more fine particles were observed.

After amplification at 500 times, samples M1, M2, M3, and M5 had similar micromorphologies without large differences, while sample M4 has a smooth but fractured surface. When observed at a magnification of 5000 times, the densities of the particles on the surfaces of samples M1, M2, M3, and M5 gradually increased, while the surface of sample M4 was smoother than the others. After amplification at 10,000 times, samples M1, M2, M3, and M5 showed more compact microstructures, while the microscopic surface of sample M4 was increasingly smoother than the others.

4 Discussion

4.1 Water-phase distributions in cement

According to the principles of NMR, the ^{1}H transverse relaxation time T_2 differs for different environments. Water in different states in the cement pastes showed specific T_2 distribution curves, which were used to characterize the freedom of the water. In the hydration processes of cement pastes, T_2 is related to the degree of confinement of the water molecules. A higher T_2 indicates greater freedom for water in the environment and less confinement. The different specific relaxation times indicate that water adopts different states during the hydration processes of the cement pastes. Gorce and Milestone (2007) found that the T_2 values of physically absorbed water and free water were distributed in the ranges of 0.1–1 ms and 1–10 ms, so 1 ms serves as the demarcation point between gel pores and capillary pores. Bohris et al. (1998) noted that before cement pastes set, there were two
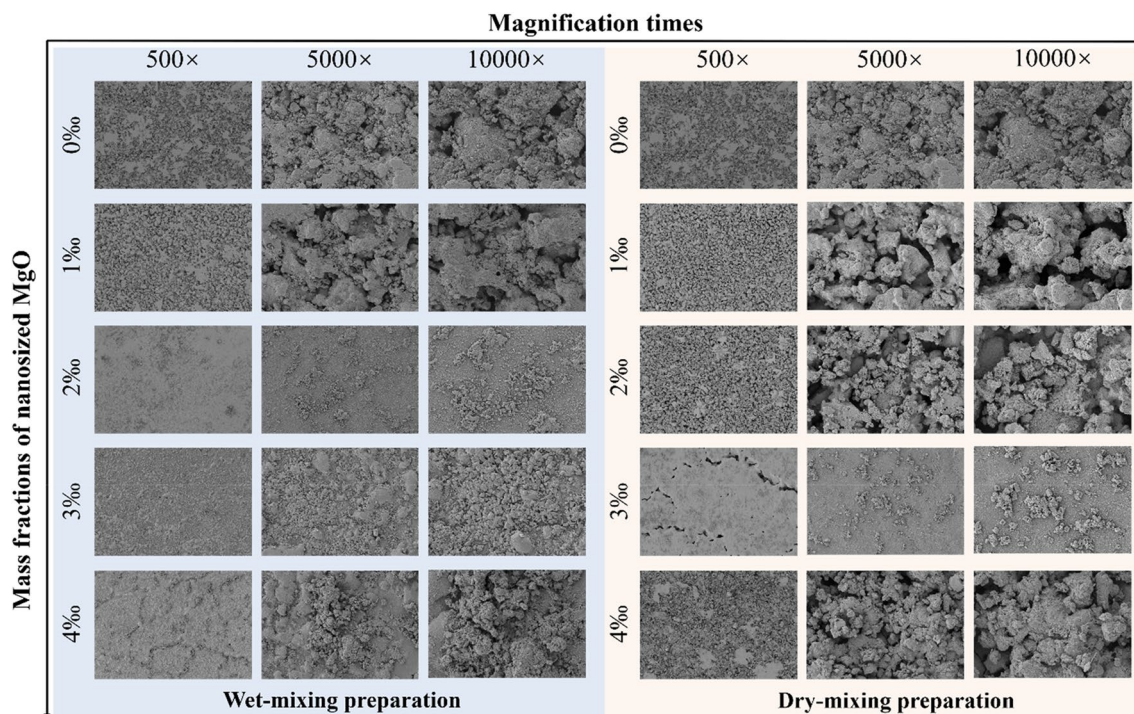
Fig. 7 Changes in micromorphologies of the hardened cement pastes

T_2 values and assigned the one at 20 μs to chemically bound water, while that at 1 ms is attributed to free water in the cement paste.

Figures 3 and 4 reveal that the relaxation peaks for cement pastes prepared with the two methods were distributed and showed the same change trends. In the initial hydration period, the relaxation peaks for the cement pastes prepared with the two methods were in the range 1–10 ms. As the hydration continued, the transverse relaxation times of cement pastes shifted toward shorter relaxation times, and the relaxation peaks finally appeared between 0.1 and 1 ms. A comparison showed that as the hydration proceeded, the relaxation peaks of the cement pastes prepared with the two methods both exhibited gradual decreases, and the peaks shifted to shorter relaxation times with reduced peak intensities and narrower relaxation ranges. The shift rate first increased and then decreased.

For the relaxation peak at 1–10 ms, the peak area constantly narrowed in the direction of longer relaxation time, while that in the short relaxation time direction enlarged as hydration continued. The relaxation peak disappeared at 720 min, which meant that the water content corresponding to the relaxation signal gradually reduced and disappeared, and then the water formed other states in the cement paste. On this basis and combined with the research of Bohris et al. (1998), the free water in the cement pastes formed other states.

The relaxation peak at 0.1–1 ms did not appear until 720 min, which indicated that water that generated the signal was not present during the initial hydration period but formed from free water in the cement paste as hydration proceeded. When the hydration duration was 720 min, the area of the relaxation peak reached the maximum value for the overall hydration process, followed by gradual shrinkage, which meant that the water producing the signal gradually formed other states with higher confinement levels. As indicated by Gorce and Milestone (2007), the physically absorbed water in the cement pastes was transformed into more confined chemically bound water.

The analysis provided above shows that there were two different water phases formed during the hydration of cement, namely, free water and physically absorbed water, and the water-phase distribution is illustrated in Fig. 8. During cement hydration, changes in the water state are correlated with the hydration process: free water is transformed into physically absorbed water and chemically bound water. Based on these correlations, the effects of the nanosized MgO on cement hydration can be determined.

4.2 Changes in the parameters of relaxation peaks

Changes in the relaxation times and intensities of the relaxation peaks for cements prepared with the two methods are shown in Figs. 9 and 10 with respect to hydration time. The figures show that the times and intensities of the relaxation
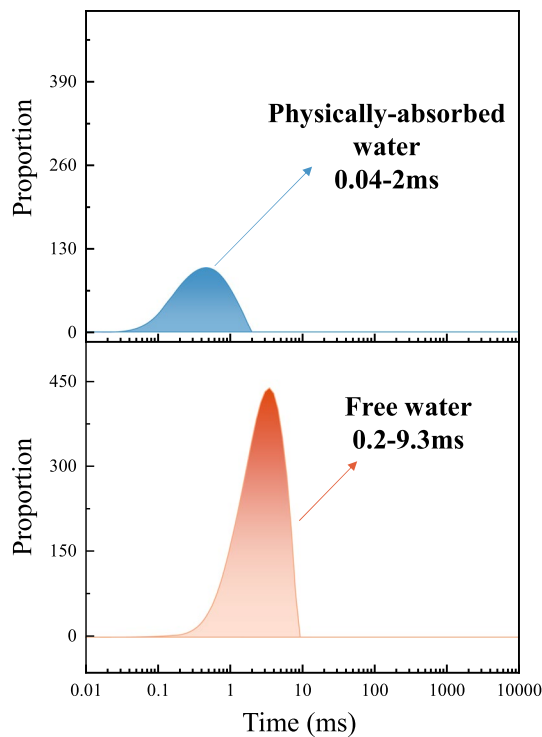
Fig. 8 Water-phase distribution in cement

peaks for the blank samples and the samples with added nanosized MgO exhibited the same change trends.

The relaxation time for the cement prepared with the wet-mixing method and modified with different mass fractions of nanosized MgO showed the same trends with hydration times, and this always significantly decreased with hydration. That is, the relaxation peak shifted leftwards. Finally, the relaxation time for the peak of sample N1 stabilized at 0.5 ms and those of samples N2–N5 stabilized at 0.4 ms. The intensities of the relaxation peaks gradually decreased with hydration. This indicated that at longer hydration times, the water in the cement pastes was more confined, and the fluidity decreased. The relaxation times of the peaks for samples N1–N5 decreased, and T_2 values of the various cement pastes decreased with the increasing mass fraction of the nanosized MgO. This indicated that changes in the values of the relaxation peaks were negatively correlated with the mass fraction of nanosized MgO. As the mass fraction of the nanosized MgO increased, the water in cement pastes was more confined, and the fluidity decreases, which facilitated cement hydration.

For cement prepared with the dry-mixing method, the relaxation time corresponding to relaxation peaks decreased with hydration. The relaxation peaks gradually shifted leftwards with hydration, and the water in the cement pastes was more confined. This indicated that with the dry-mixing preparation, free water was transformed into physically absorbed water and chemically bound water with higher degrees of confinement during hydration. The intensities of the relaxation peaks for the cement pastes prepared with the dry-mixing method decreased with increased mass fractions of the nanosized MgO, and they were negatively correlated with the hydration time. This suggested that the degree of hydration rose and the values of the relaxation peaks of cement pastes declined with the increased in the hydration time. After 720 min of hydration, the values of the relaxation peaks of cement pastes gradually decreased with increasing mass fraction of the nanosized MgO. When the hydration time was 720–1800
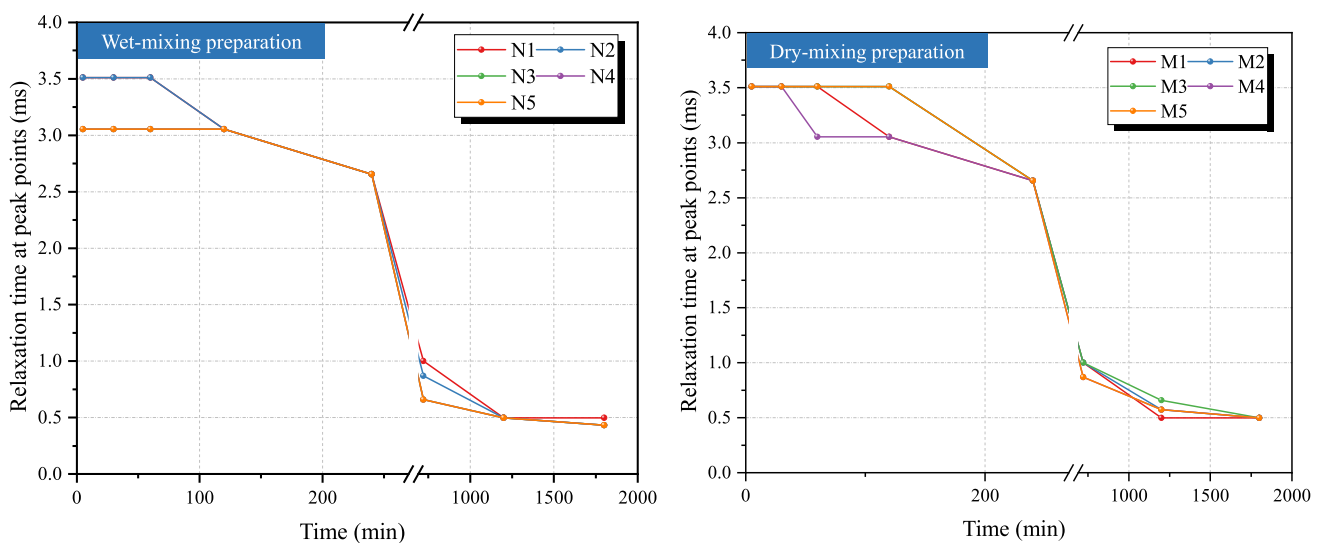

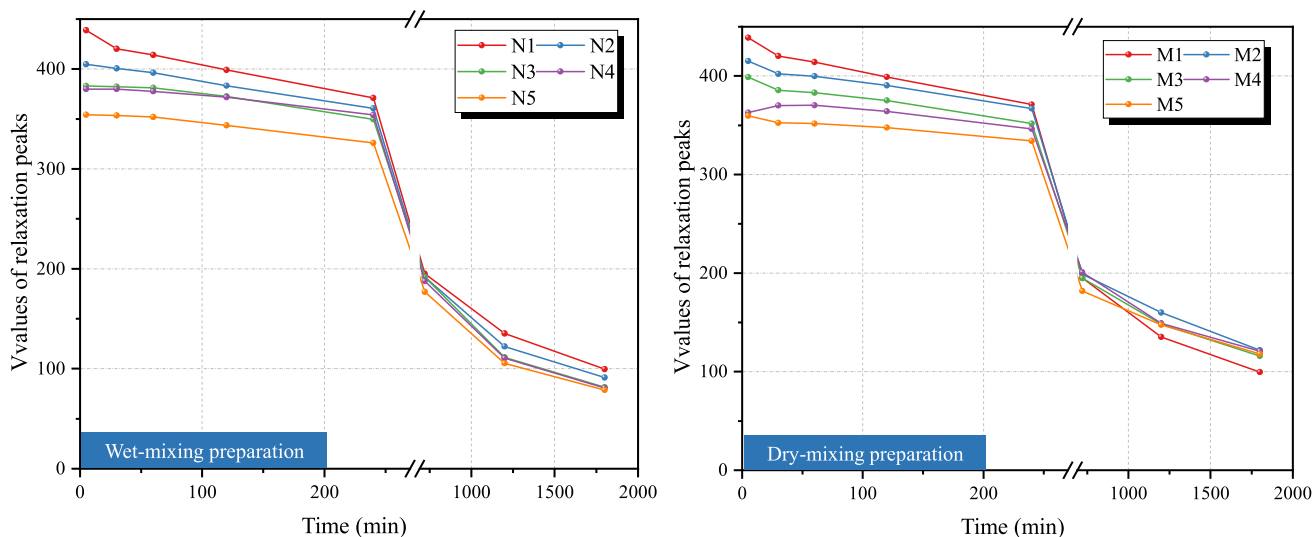**Fig. 9** Relaxation times at the peak points as a function of hydration time

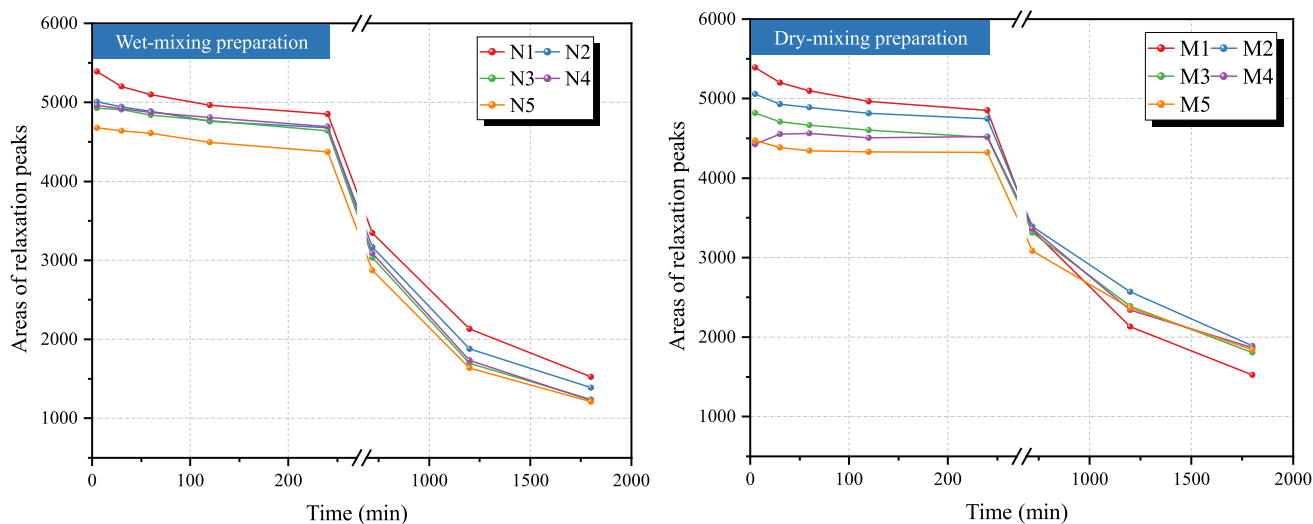**Fig. 10** Relaxation peaks as a function of hydration time

Fig. 11 Areas of the relaxation peaks for the cements versus hydration time

min, the mass fraction of the nanosized MgO did not show an obvious correlation with the intensities of the relaxation peaks, which suggested that at this stage, the effect of the nanosized MgO on cement hydration was inconsistent for the dry-mixing method.

The areas of the relaxation peaks of cement pastes prepared using the two methods are shown in Fig. 11 as a function of the hydration time. As shown in the figure, the areas of relaxation peaks for Groups N1–N5 prepared with the wet-mixing method reached a maximum after 5 min of hydration. When the hydration time is in the range of 30–240 min, the areas of the relaxation peaks for cement pastes N1–N5 gradually narrowed with increasing hydration time, although not greatly. As the hydration continued

for 240 to 1200 min, the areas of the relaxation peaks for cement pastes N1–N5 decreased significantly. If the hydration time was in the range 1200 to 1800 min, the areas of the relaxation peaks narrowed slowly and gradually stabilized. This indicated reduced fluidity of the cement pastes with increasing hydration time. However, the rates for fluidity loss for the cement pastes differed in the different periods. This was because within 240 min of hydration, the cement was fully hydrated, during which free water was consumed and its content gradually decreased; the hydration products were produced and adhered to the surfaces of the cement particles, which to slowed or hindered cement hydration. In addition, particles on the surfaces of the cement particles and the nanosized MgO dissolved

in the period, which reduced particle aggregation and reduced the fluidity of the cement paste. This explains the slight reductions in the macroscopic fluidities of the cement pastes in the period.

As the mass fraction of the nanosized MgO increased, the areas of the relaxation peaks for the cement pastes decreased (while not greatly) during the various hydration periods. This meant that with increased mass fraction for the nanosized MgO, the fluidity of the cement pastes was weakened gradually and slightly overall. The reductions in the fluidities of the cement pastes due to the increased mass fractions of the nanosized MgO were mainly attributed to the following factors:

(1) There are pores in the MgO aggregates. Due to the capillary effects of the internal pores, a small part of the free water was absorbed and converted into capillary water in the nanosized MgO. This explains why compared with the control N1, the contents of free water were always slightly reduced in cement pastes N2–N5 containing nanosized MgO, and the fluidity also slightly decreased. (2) Because the MgO had small particles, the specific surface areas were larger than those of the cement particles, and it required more water for wetting. According to Zhang, this reduced the fluidity of the cement paste. (3) Due to the high activity, nanosized MgO reacted rapidly with water and competed effectively with the cement. Therefore, as more nanosized MgO was added, more water was captured and the fluidity of the cement paste was reduced.

The same change trend was observed for samples M1–M5 prepared with the dry-mixing method. As cement hydration proceeded, the areas of the relaxation peaks for the various cement pastes gradually narrowed, which indicated that the fluidities of the cement pastes gradually decreased as hydration continued. Within 240 min of hydration, the areas of the relaxation peaks for cement pastes M1–M5 decreased gently. As hydration continued for 240–1200 min, the areas of relaxation peaks for cement pastes M1–M5 narrowed greatly. When the hydration time was 1200–1800 min, the reductions in the peak areas became gentle again. This indicated that the fluidities of the cement pastes decreased slightly within 240 min of hydration, while it was mainly lost for hydration times of 240–1200 min, during which the cement pastes gradually set. Within 720 min of hydration, the areas of the relaxation peaks for the cement pastes narrowed with the increased mass fractions of the nanosized MgO. When the hydration time was 720–1800 min, the mass fraction of the nanosized MgO was not obviously correlated with the areas of the relaxation peaks, which indicated that nanosized MgO had an inconsistent effect on hydration of the cements prepared with the dry-mixing method.

## 4.3 Influence of nanosized MgO on the hydration process of cement

By analysing changes in the total relaxation signals of the cements prepared with the two methods, the variations in the relaxation signals were found to exhibit three stages, the induction, acceleration, and deceleration periods. Among them, the induction period is below 240 min, the acceleration period is between 240 and 720 min, and the deceleration period is above 720 min, which are highly consistent with the multi-stage characteristics defined by Xu et al. obtained from the variation of the anti-resonance frequency and anti-resonance resistance value of the sensor with the cement hydration reaction time (Xu et al. 2011).

(1) Induction period: the total relaxation signals of the cement pastes decreased with increasing nanosized MgO content. Because the dissolution of cement clinker in the induction period mainly involves the dissolution of tricalcium silicate (C_3S), the reaction for the dissolution process is (Nicoleau and Nonat 2016):

$$Ca_3SiO_5 + 5H_2O \rightarrow 3Ca^{2+} + 6OH^- + H_4SiO_4 \quad (1)$$
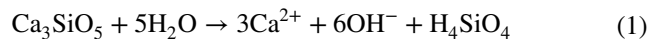
The demand for hydroxyl ions increases during hydration of the nanosized MgO, which accelerates the dissolution of C_3S. When the mass fraction of nanosized MgO increases, more hydroxyl ions are needed, and more water is consumed. This is shown as a reduction of the total relaxation signals for the cement pastes with increased contents of the nanosized MgO and increased hydration with increases proportions of the nanosized MgO. Calcium hydroxide and tobermorite begin to nucleate, and the nanosized MgO is hydrated to produce smaller nanosized magnesium hydroxide ($Mg(OH)_2$) particles, which function as nucleation sites for cement hydration. Increased mass fractions of the nanosized MgO provides more nucleation sites for calcium hydroxide and tobermorite, thus promoting cement hydration. As a result, the total relaxation signals of the cement pastes decrease with increasing nanosized MgO content.

(2) Acceleration period: as the induction period ends, the concentrations of various ions in the aqueous solution increase. Due to the permeation pressure, the barrier layers of the hydration products on the surfaces of the cement particles are ruptured so water comes into contact with the surfaces of the cement particles, which increases the hydration rate. In this way, hydration enters the acceleration period, during which the hydration product tobermorite is formed rapidly. The reaction for the precipitation process is as follows (Jansen et al. 2012):

$$xCa^{2+} + 2xOH^- + H_4SiO_4 \rightarrow (CaO)_x - (SiO_2) - (H_2O)_b$$
$$+ (2 + x - b)H_2O$$

$$(2)$$
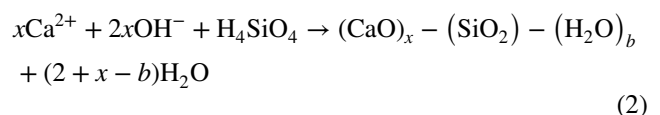
In this stage, the change rate for the total relaxation signals of water rises and reaches the maximum value for the whole hydration process. This indicates that as cement hydration accelerates, the amounts of hydration products increase rapidly, the porosity decreases, and cement pastes begin to set and lose plasticity. As the mass fraction of the nanosized MgO rises, more water is consumed in hydration of the nanosized MgO, which increases the concentration of calcium ions in the aqueous solution and promotes cement hydration.

(3) Deceleration period: many hydration products have been produced in the cement paste. The formation rate of the hydration products decreases, and the structure becomes more compact, such that diffusion of the ions and water are inhibited, and the total relaxation signals change slowly. In this period, the nanosized MgO is still constantly hydrated, so the hydration rate rises with increases in the mass fraction of the nanosized MgO.

The above analysis reveals that higher contents of the nanosized MgO accelerate hydration and increase the degree of hydration. The nanosized MgO promotes cement hydration, and this effect is enhanced with increased mass fractions of the nanosized MgO (Fig. 12).

4.4 Effects of preparation methods on hydration of cements modified with nanosized MgO

4.4.1 Hydration process

According to the above, the T_2 distribution curves of samples N1–N5 changed in a similar manner to those of M1–M5, which implied consistent state transformations for water in the cements prepared with both the wet-mixing and dry-mixing methods. Free water and physically absorbed water were

both present during hydration of the cement pastes containing different mass fractions of nanosized MgO and prepared using different methods. In the hydration process of cement, the degree of water confinement gradually improved, and the different preparation methods did not affect the water transformations in the cement.

The T_2 distribution curves of the cement pastes prepared with the wet-mixing and dry-mixing methods showed similar change trends, while their amplitudes differed greatly. To indicate clearly the effect of the preparation method on the hydration process, the shift rate was defined as the change in the relaxation peak position per unit time to reflect changes in the contents of different states of water in the cement pastes. Moreover, β was defined as a shape index for the relaxation
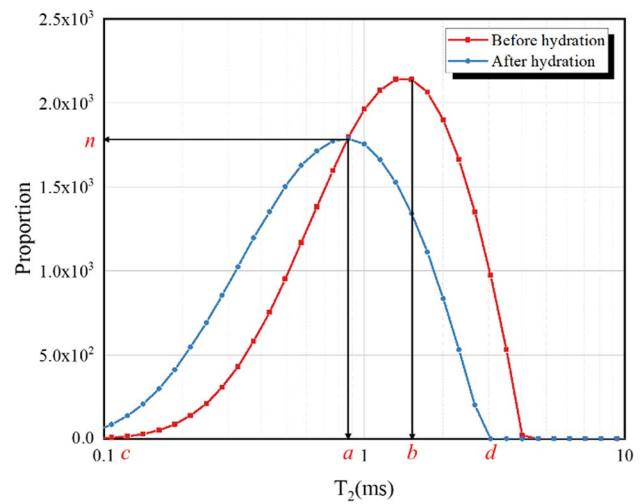

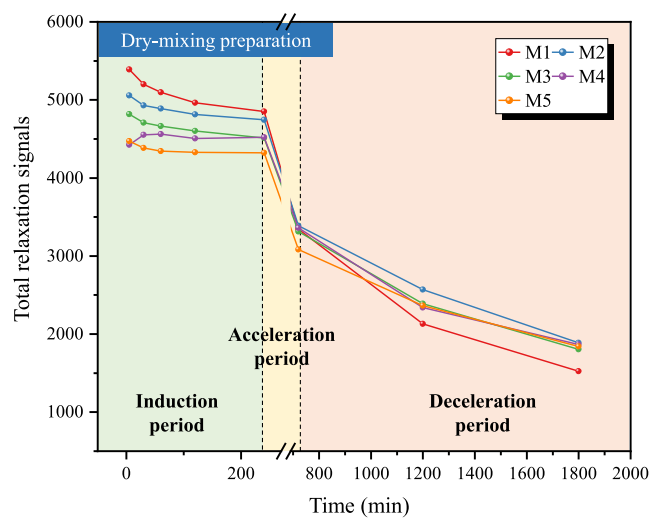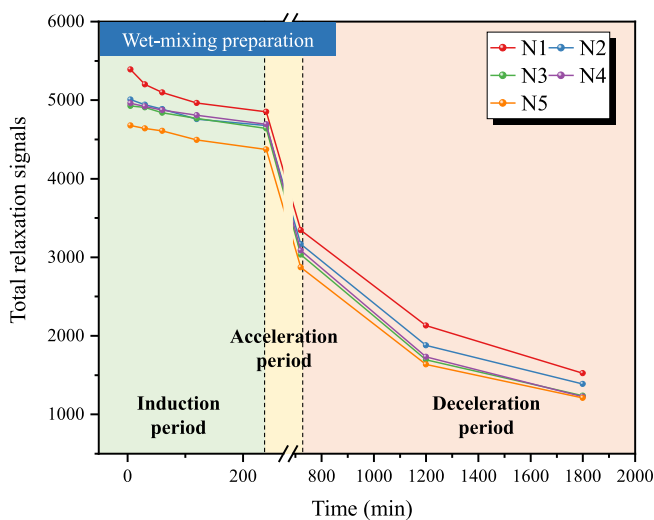**Fig. 13** Schematic diagrams of the T_2 peaks

Fig. 12 Hydration stages of cement

peaks to characterize the external environments for all states of water in the cement pastes. Figure 13 shows the T_2 distribution curves determined for the same cement paste before and after hydration for several hours.

$$\alpha = \frac{b - a}{t} \tag{3}$$

$$\beta = \frac{n}{d - c} \tag{4}$$

where, b and a separately denote the position of the T_2 peak before and after hydration of the cement; t is the hydration time; n is the relaxation signal determined after hydration for several hours; and c and d separately denote the starting and ending times of the peaks measured after hydration for several hours.

The effects of the preparation methods on the shape indexes of the cement relaxation peaks are displayed in Fig. 14. The shape indices of the relaxation peaks for cements prepared with different methods exhibited the same change trends. The shape index increased at first and then

decreased with the increased hydration time. Within 720 min of hydration, the shape indexes for the relaxation peaks of cement pastes prepared with the dry-mixing method were smaller than those of cement pastes prepared with the wet-mixing method and the same mass fraction of nanosized MgO. This indicated that within 720 min of hydration, the nanosized MgO enhanced hydration of the cement prepared with the wet-mixing method more effectively than that of the cement prepared with the dry-mixing method. When the hydration time was 720–1800 min, the nanosized MgO still promoted hydration of the cement paste prepared with the wet-mixing method, but the promotion effect of the nanosized MgO on cement hydration was inconsistent for cement pastes prepared with the dry-mixing method. However, at this stage, the shape indexes of the relaxation peaks for cement pastes prepared with the dry-mixing method and the same mass fraction of nanosized MgO were larger than those of cement pastes prepared with the wet-mixing method. This indicated that the nanosized MgO had a stronger promotion
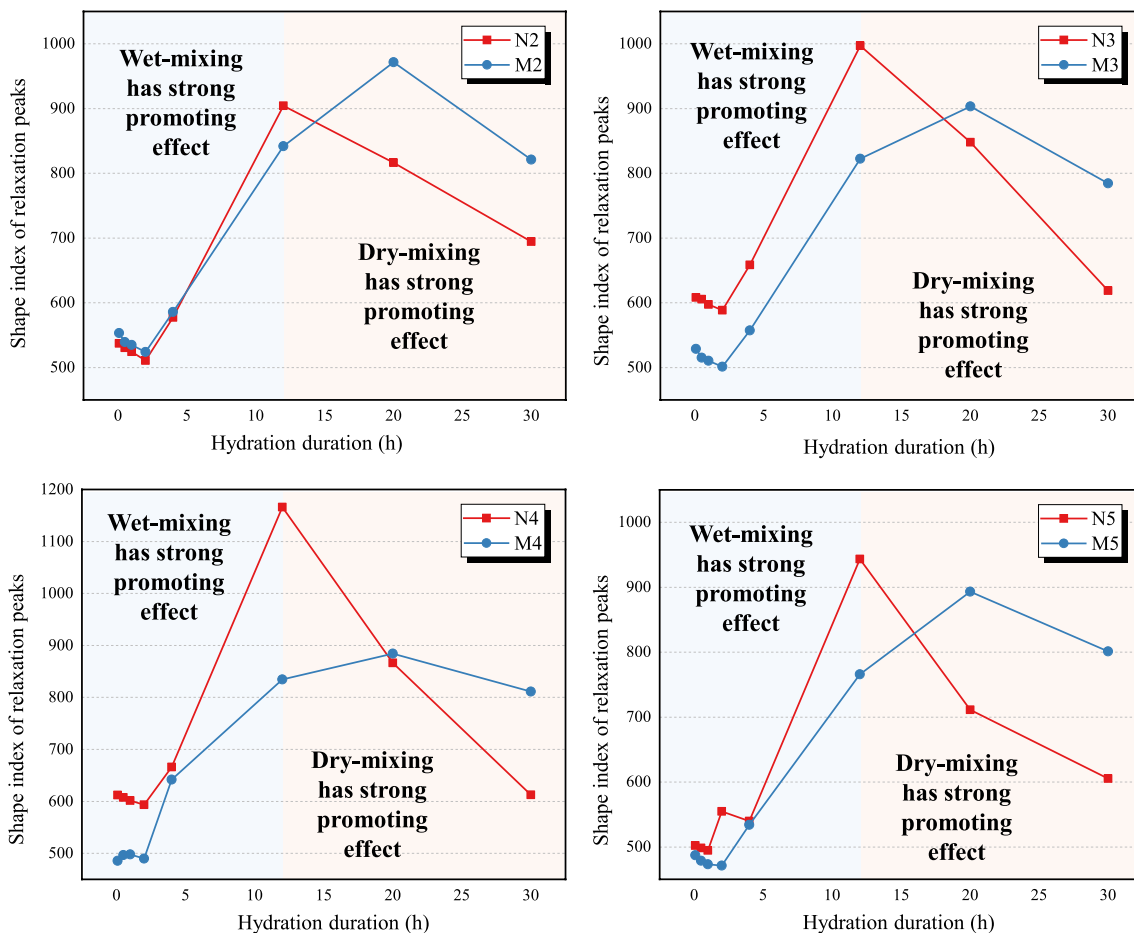

Fig. 14 Effects of preparation methods on the shape indexes for the relaxation peaks of the cement pastes
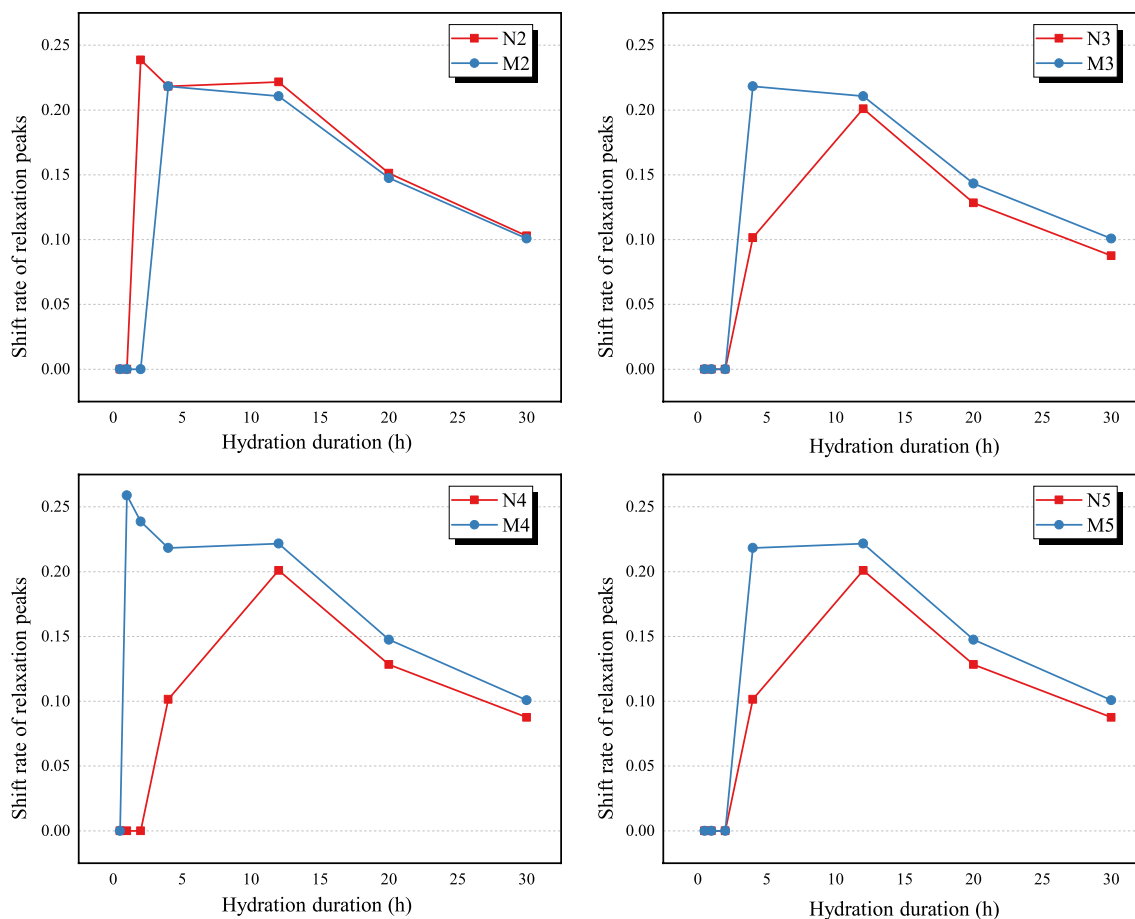
Fig. 15 Effects of preparation methods on the shift rates of the relaxation peaks for cement pastes
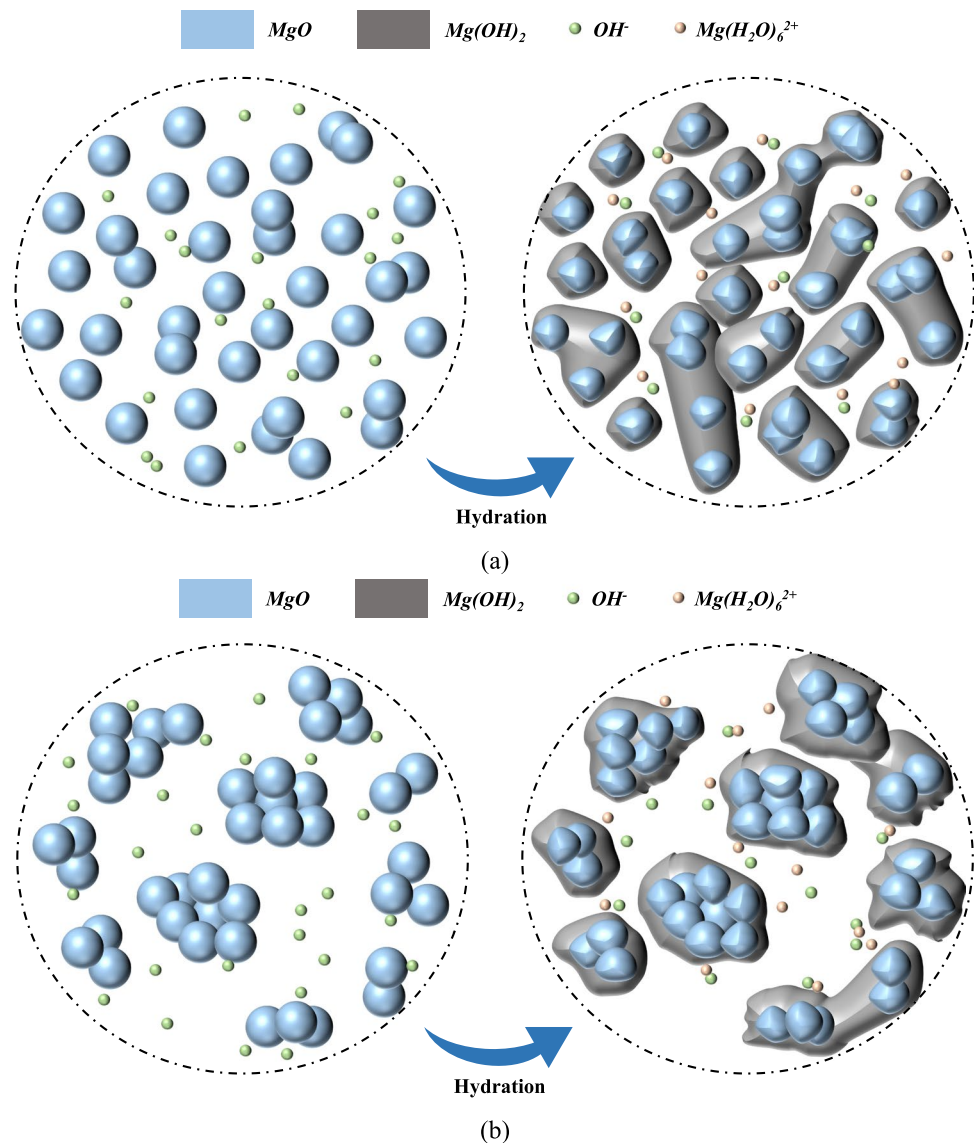
effect on cement hydration for the dry-mixing method than the wet-mixing method.

The effects of the preparation methods on the shift rates of the relaxation peaks for the cement pastes are shown in Fig. 15. The shift rates for the relaxation peaks of the cement pastes prepared with different methods changed with the same trends. The shift rate increased at first and then decreased with increasing hydration time. Based on a theoretical analysis of cement hydration, the shift rate was found to gradually rise in the induction and acceleration periods of the cement pastes, while it gradually declined in the deceleration period with increased hydration time. Because the shift rate indicates the looseness of the flocculent structures in cement pastes, that is, the degree of free water confinement, cement pastes prepared with the wet-mixing method show lower shift rates than those prepared with the dry-mixing method. This is because the flocculent structures exist for longer periods of time in the cement pastes prepared with the wet-mixing method, in which the degree of confinement for the water in the flocculent structures changes slightly. The free water is transformed into chemically bound water

at a slower rate, and the content of free water in the cement paste changes slightly.

The effects of the nanosized MgO on hydration of cements prepared with the different methods were analysed, which revealed the mechanism for hydration of the nanosized MgO particles for the different preparation methods, as shown in Fig. 16. An ultrasonic instrument was used for ultrasonic dispersion of the nanosized MgO in the wet-mixing preparation, so the nanosized MgO was dispersed uniformly and with little aggregation (Fig. 16a). Due to uniform dispersion of the nanosized MgO, the surface area of the reaction was enlarged, which enabled reactions between the nanosized MgO and OH^- and produces many $Mg(OH)_2$ particles. These particles provided many nucleation sites for the cement hydration products, thus accelerating hydration. For the dry-mixing preparation, the nanosized MgO was dispersed nonuniformly and underwent aggregation (Fig. 16b). When the same mass fraction of nanosized MgO was added, the nanosized MgO in the dry-mixing preparation had a smaller surface area for the reaction than that of the wet-mixing preparation. Only few nanosized MgO particles on the surfaces of the aggregated clusters participated in hydration to form $Mg(OH)_2$, so only a

Fig. 16 Mechanisms for the effects of nanosized MgO on hydration **a** Wet-mixing preparation **b** Dry-mixing preparation

(a)

(b)

few nucleation sites were provided for the hydration products. As a result, the effect of the nanosized MgO during hydration of the cement paste was inconsistent when using the dry-mixing preparation method.

4.4.2 Effects of the preparation methods on the surface porosities of the cements

To study the effect of the preparation method on the surface porosity of the cement, Avizo and Photoshop were used to quantitatively analyse the microstructures of the pores in the SEM images of the cement. The surface porosity indicates the ratio of fracture areas to the total area in SEM secondary electron images. It can be seen from the SEM images in Fig. 7 that the pores were dark and had a low grey value (approximately 0) because they were sunken. An appropriate grey threshold was selected for processing Fig. 7 into

binary digital images that reflected the pores and fractures, as displayed in Fig. 17 (the black areas are pores and microfractures). The proportion of black pixels was calculated using Avizo, so the changes in the surface porosities of the different cement pastes were determined (Fig. 17).

As shown in Fig. 17, the surface porosity of cement decreased at first and then increased with increasing mass fraction of the nanosized MgO for the wet-mixing preparation method, as evinced by the decreasing and then increasing trends for the area and number of black regions in the binary images. According to the mechanism described above for hydration of the nanosized MgO in the wet-mixing preparation, when the mass fraction of the nanosized MgO was in the range 0‰–2‰, the hydration products on cement surfaces were compact with uniformly distributed folds and few pores, so the surfaces were relatively smooth. If the mass fraction of the nanosized MgO reached 3‰,
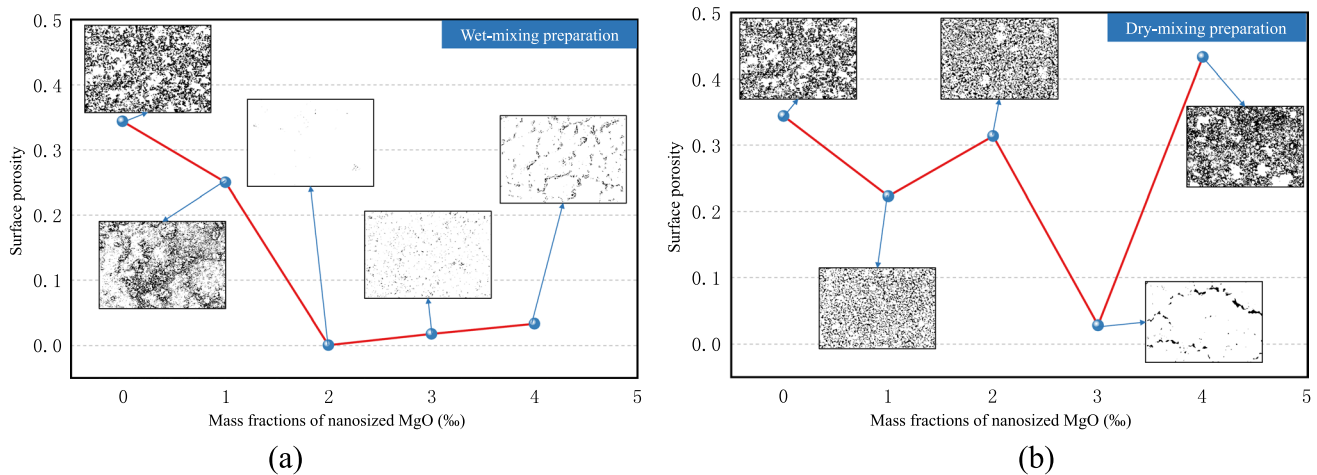
Fig. 17 Changes observed in the surface porosities of cements modified with nanosized MgO **a** Wet-mixing preparation **b** Dry-mixing preparation

some hydration products covered the smooth surfaces of the cement due to the excellent expansibility of the nanosized MgO, which resulted in the appearance of fine pores and cracks, as evinced by the slight increasing trend for the surface porosity of the cement. Overall, the surface porosity of the cement modified with nanosized MgO and prepared via the wet-mixing method was lower than that of pure cement, indicating that the wet-mixing method effectively increased the compactness of the cement. In comparison, the surface porosity of the cement prepared with the dry-mixing method fluctuated with the mass fraction of the nanosized MgO, and the cement surfaces were rough and exhibited fine fractures on some surfaces. According to the mechanism described above for hydration of the nanosized MgO in the dry-mixing preparation, the preparation method may cause aggregation of the cement hydration products, many fractures and pores on the cement surfaces, and therefore relatively low compactness. Generally, the two preparation methods both reduce the surface porosity of the cement, while the wet-mixing preparation method is more effective and consistent in improving the compactness of cement than the dry-mixing preparation.

5 Conclusions

NMR and SEM were used to explore the effects of nanosized MgO on the hydration of cement pastes prepared with different methods. Changes in the hydration reactions and hydration products of the cement pastes modified with nanosized MgO and prepared using different methods were revealed. The effects of nanosized MgO on the hydration of cements prepared with the different methods were clarified, and the mechanisms for hydration of the nanosized MgO with the

different preparation methods were revealed. The following conclusions were reached:

(1) The T_2 distribution curves for cement pastes in the 0.1–1 ms and 1–10 ms ranges represented physically absorbed water and free water in the cement pastes. An increased mass fraction for the nanosized MgO facilitated cement hydration of cement. A higher nanosized MgO mass fraction enhanced the rate and extent of cement hydration. Compared with the dry-mixing preparation, the wet-mixing method exhibited more water-phase transformations in the cement pastes.

(2) The nanosized MgO promoted the hydration induction, acceleration, and deceleration periods for the wet-mixing method. It accelerated cement hydration and rendered the microstructures of the cement pastes more compact. In comparison, the nanosized MgO promoted the hydration induction period for cement prepared with the dry-mixing method, and the effect was less significant than that of the wet-mixing preparation; the effects of nanosized MgO on the acceleration and deceleration periods of cement hydration were inconsistent due to stirring and dispersion effects.

(3) The nanosized MgO was uniformly dispersed when using the wet-mixing preparation method. This enlarged the surface area of the reaction and enhanced the reaction between the nanosized MgO and OH^-, which produced many $Mg(OH)_2$ particles that provided numerous nucleation sites for formation of the cement hydration products, thus accelerating hydration. In the dry-mixing preparation, the nanosized MgO was dispersed nonuniformly and aggregated. Only a small number of nanosized MgO particles on the aggregated clusters participated in hydration to form $Mg(OH)_2$ par-

ticles. As a result, only a small number of nucleation sites were provided for the cement hydration products, which resulted in inconsistent effects of the nanosized MgO in hydration of the cement pastes prepared with the dry-mixing method.

(4) The surface porosity of the cement decreased at first and then increased with increasing mass fraction of the nanosized MgO when using the wet-mixing preparation method. The hydration products on the surface of the cement were compact when using the preparation method, with uniformly distributed folds, a few pores, and smooth surfaces. When using the dry-mixing preparation method, the surface porosity of the cement fluctuated with the mass fraction of the nanosized MgO, and the cement surface was rough, with fine fractures on some surfaces. The two preparation methods both reduced the surface porosity of the cement, while the wet-mixing preparation method was more effective and stable than the dry-mixing method in improving the compactness of the cement.

References

Aly M, Hashmi MSJ, Olabi AG (2011) Effect of nano clay particles on mechanical, thermal and physical behaviours of waste-glass cement mortars. Mater Sci Eng A 528:7991–7998. https://doi.org/10.1016/j.msea.2011.07.058

Behroozmand AA, Keating K, Auken E (2015) A review of the principles and applications of the NMR technique for near-surface characterization. Surv Geophys 36:27–85. https://doi.org/10.1007/s10712-014-9304-0

Bohris AJ, Goerke U, McDonald PJ et al (1998) A broad line NMR and MRI study of water and water transport in Portland cement pastes. Magn Reson Imaging 16:455–461. https://doi.org/10.1016/S0730-725X(98)00072-1

Brownstein K, Tarr C (1979) Importance of classical diffusion in NMR-studies of water in biological cells. Phys Rev A 19:2446–2453. https://doi.org/10.1103/PhysRevA.19.2446

Farzadnia N, Abang Ali AA, Demirboga R (2013a) Characterization of high strength mortars with nano alumina at elevated temperatures. Cem Concr Res 54:43–54. https://doi.org/10.1016/j.cemconres.2013.08.003

Farzadnia N, Abang Ali AA, Demirboga R, Anwar MP (2013b) Effect of halloysite nanoclay on mechanical properties, thermal behavior and microstructure of cement mortars. Cem Concr Res 48:97–104. https://doi.org/10.1016/j.cemconres.2013.03.005

Farzadnia N, Abang Ali AA, Demirboga R, Anwar MP (2013c) Characterization of high strength mortars with nano Titania at elevated temperatures. Constr Build Mater 43:469–479. https://doi.org/10.1016/j.conbuildmat.2013.02.044

Gao L, Ren Z, Yu X (2015) Experimental study of nanometer magnesium oxide-modified clay. Soil Mech Found Eng 52:218–224. https://doi.org/10.1007/s11204-015-9331-y

Ge Z, Mei X, Lu Y (2015) Optimization and application of sealing material and sealing length for hydraulic fracturing borehole in underground coal mines. Arab J Geosci 8:3477–3490. https://doi.org/10.1007/s12517-014-1488-6

Gorce J-P, Milestone NB (2007) Probing the microstructure and water phases in composite cement blends. Cement Concrete Res 37:310–318. https://doi.org/10.1016/j.cemconres.2006.10.007

Hakamy A, Shaikh F, Low IM (2013) Microstructures and mechanical properties of hemp fabric reinforced organoclay–cement nanocomposites. Constr Build Mater 49:298–307. https://doi.org/10.1016/j.conbuildmat.2013.08.028

Holly R, Reardon EJ, Hansson CM, Peemoeller H (2007) Proton spin-spin relaxation study of the effect of temperature on white cement hydration. J Am Ceram Soc 90:570–577. https://doi.org/10.1111/j.1551-2916.2006.01422.x

Horszczaruk E, Aleksandrzak M, Cendrowski K, et al (2020) Mechanical properties cement based composites modified with nano-Fe3O4/SiO2. Constr Build Mater 251:118945. https://doi.org/10.1016/j.conbuildmat.2020.118945

Hou P, Cai Y, Cheng X (2017) Effects of the hydration reactivity of ultrafine magnesium oxide on cement-based materials. Mag Concr Res 69:1135–1145. https://doi.org/10.1680/jmacr.16.00212

Jansen D, Goetz-Neunhoeffer F, Lothenbach B, Neubauer J (2012) The early hydration of Ordinary Portland Cement (OPC): An approach comparing measured heat flow with calculated heat flow from QXRD. Cem Concr Res 42:134–138. https://doi.org/10.1016/j.cemconres.2011.09.001

Kritikaki A, Tsetsekou A (2009) Fabrication of porous alumina ceramics from powder mixtures with sol–gel derived nanometer alumina: Effect of mixing method. J Eur Ceram Soc 29:1603–1611. https://doi.org/10.1016/j.jeurceramsoc.2008.10.011

Liu X, Chen L, Liu A, Wang X (2012) Effect of nano-CaCO₃ on properties of cement paste. Energy Procedia 16:991–996. https://doi.org/10.1016/j.egypro.2012.01.158

Liu Q, Cheng Y, Yuan L (2014) A new effective method and new materials for high sealing performance of cross-measure CMM drainage boreholes. J Nat Gas Sci Eng 21:805–813. https://doi.org/10.1016/j.jngse.2014.10.023

Lu Y, Zhang Y, Tang J, Yao Q (2022) Switching mechanism and optimisation research on a pressure-attitude adaptive adjusting coal seam water jet slotter. Int J Min Sci Tech 32:1167–1179

Ma B, Ma M, Shen X et al (2014) Compatibility between a polycarboxylate superplasticizer and the belite-rich sulfoaluminate cement: setting time and the hydration properties. Constr Build Mater 51:47–54. https://doi.org/10.1016/j.conbuildmat.2013.10.028

Moradpour R, Taheri-Nassaj E, Parhizkar T, Ghodsian M (2013) The effects of nanoscale expansive agents on the mechanical properties of non-shrink cement-based composites: the influence of

nano-MgO addition. Compos Part B Eng 55:193–202. https://doi.org/10.1016/j.compositesb.2013.06.033

Nazari A, Riahi S (2011) The effects of TiO_2 nanoparticles on physical, thermal and mechanical properties of concrete using ground granulated blast furnace slag as binder. Mater Sci Eng A 528:2085–2092. https://doi.org/10.1016/j.msea.2010.11.070

Nestle N (2004) NMR relaxometry study of cement hydration in the presence of different oxidic fine fraction materials. Solid State Nucl Magn Reson 25:80–83. https://doi.org/10.1016/j.ssnmr.2003.05.003

Nicoleau L, Nonat A (2016) A new view on the kinetics of tricalcium silicate hydration. Cem Concr Res 86:1–11. https://doi.org/10.1016/j.cemconres.2016.04.009

Ran Q, Liang Y, Zou Q (2023a) Experimental investigation on mechanical characteristics of red sandstone under graded cyclic loading and its inspirations for stability of overlying strata. Geomech Geophys Geo-Energy Geo-Resour 9:11. https://doi.org/10.1007/s40948-023-00555-x

Ran Q, Liang Y, Zou Q (2023b) Characteristics of mining-induced fractures under inclined coal seam group multiple mining and implications for gas migration. Nat Resour Res. https://doi.org/10.1007/s11053-023-10199-z

Ren Z, Liu Y, Yuan L (2021) Optimizing the content of nano-SiO_2, nano-TiO2 and nano-$CaCO_3$ in Portland cement paste by response surface methodology. J Build Eng 35:102073. https://doi.org/10.1016/j.jobe.2020.102073

Sato T, Diallo F (2018) Seeding effect of nano-$CaCO_3$ on the hydration of tricalcium silicate. Transp Res Rec. https://doi.org/10.3141/2141-11

Simina M, Molnar L, Manea D, Ardelean I (2012) Monitoring the air influence on cement-lime mortar hydration using low-field nuclear magnetic resonance relaxometry. Appl Magn Reson 43:443–450. https://doi.org/10.1007/s00723-012-0389-7

Sun Z, Voigt T, Shah SP (2006) Rheometric and ultrasonic investigations of viscoelastic properties of fresh Portland cement pastes. Cem Concr Res 36:278–287. https://doi.org/10.1016/j.cemconres.2005.08.007

Supit SWM, Shaikh FUA (2014) Effect of nano-$CaCO_3$ on compressive strength development of high volume fly ash mortars and concretes. J Adv Concr Technol 12:178–186. https://doi.org/10.3151/jact.12.178

Tavassolian N, Li M, Vassiliou CC, Cima MJ (2014) A novel magnetic relaxation-based platform for hydration monitoring. IEEE Sens J. https://doi.org/10.1109/JSEN.2014.2319053

Wang LH, Duan YF (2013) Study on the quick hardening cement-based grouting material's modification by nano-materials. Appl Mech Mater 357–360:718–723. https://doi.org/10.4028/www.scientific.net/AMM.357-360.718

Wang H, Yao Y, Liu D (2016) Fault-sealing capability and its impact on coalbed methane distribution in the Zhengzhuang field, southern Qinshui Basin, North China. J Nat Gas Sci Eng 28:613–625. https://doi.org/10.1016/j.jngse.2015.12.036

Xiao L, Li Z (2008) Early-age hydration of fresh concrete monitored by non-contact electrical resistivity measurement. Cem Concr Res 38:312–319. https://doi.org/10.1016/j.cemconres.2007.09.027

Xie H, Wu L, Zheng D (2019) Prediction on the energy consumption and coal demand of China in 2025. J China Coal Soc 44:1949–1960. https://doi.org/10.13225/j.cnki.jccs.2019.0585

Xu DY, Qin L, Huang SF, Cheng X (2011) An exploration of 1–3 cement/epoxy resin based piezoelectric composite in cement hydration reaction process monitoring. Adv Mater Res 306–307:839–843. https://doi.org/10.4028/www.scientific.net/AMR.306-307.839

Yan L (2014) Research progress on application of new cement-based grouting materials in coal mine underground. Silicate Bull 33(01):97–102. https://doi.org/10.16552/j.cnki.issn1001-1625.2014.01.035

Ye Q, Yu K, Zhang Z (2015) Expansion of ordinary Portland cement paste varied with nano-MgO. Constr Build Mater 78:189–193. https://doi.org/10.1016/j.conbuildmat.2014.12.113

Zhai C, Xiang X, Xu J, Wu S (2016) The characteristics and main influencing factors affecting coal and gas outbursts in Chinese Pingdingshan mining region. Nat Hazards 82:507–530. https://doi.org/10.1007/s11069-016-2195-2

Zhang H, He Y, Tang C, Ahmad B, Han L (2009) Application of an improved flow-stress-damage model to the criticality assessment of water inrush in a mine: a case study. Rock Mech Rock Eng 42:911–930. https://doi.org/10.1007/s00603-008-0004-2

Zou Q, Chen Z, Cheng Z, Liang Y, Xu W, Wen P, Zhang B, Liu H, Kong F (2022) Evaluation and intelligent deployment of coal and coalbed methane coupling coordinated exploitation based on Bayesian network and cuckoo search. Int J Min Sci Tech 32:1315–1328. https://doi.org/10.1016/j.ijmst.2022.11.002

Zou Q, Huo Z, Zhang T, Jiang C, Liang J (2023) Surface deposition characteristics of water-based SiO_2 nanofluids on coal. Fuel 340:127489. https://doi.org/10.1016/j.fuel.2023.127489